EUROPHYSICS LETTERS 15 February 2001

Europhys. Lett., **53** (4), pp. 518–524 (2001)

Electrohydrodynamic instabilities in polymer films

E. SCHÄFFER[1,2], T. THURN-ALBRECHT[3](*), T. P. RUSSELL[3] and U. STEINER[1](**)

[1] *Department of Polymer Chemistry, Materials Science Center, University of Groningen Nijenborgh 4, NL-9747 AG Groningen, The Netherlands*

[2] *Fakultät für Physik, Universität Konstanz - D-78456 Konstanz, Germany*

[3] *Polymer Science and Engineering Department, University of Massachusetts at Amherst Amherst, MA 01003, USA*

(received 2 August 2000; accepted in final form 4 December 2000)

PACS. 68.10.-m – Fluid surfaces and fluid-fluid interfaces.
PACS. 47.20.Ma – Interfacial instability.
PACS. 47.65.+a – Magnetohydrodynamics and electrohydrodynamics.

Abstract. – We have studied the influence of electric fields on highly viscous polymer films. An electrohydrodynamic (EHD) instability causes a wave pattern with a characteristic wavelength λ, leading to an array of polymer columns which span the gap of a capacitor device. When represented as a master curve, the data is quantitatively described by an EHD model, without any adjustable parameters. Our results suggest that EHD experiments using polymer films are well suited to study non-equilibrium pattern formation in quasi–two-dimensional systems.

The physical basis for the deformation of a liquid surface by an electric field has been known for more than a century [1]. EHD surface instabilities have been studied using a variety of liquids. In transformer oils, instabilities lower the critical voltage for dielectric breakdown [2], in thermoplasts, they cause a surface roughening ("frosting") [1] and in liquid helium they give rise to surface waves ("ripplons") [3].

The first theories on the rupture of liquid films by an electric field [2] led to an extensive investigation of EHD instabilities [4,5]. Two qualitatively different cases can be distinguished [1–6]: 1) Free charges at a liquid-air or liquid-liquid interface. This effect is achieved, for example, by exposing a thermoplastic surface to a discharge, or by the accumulation of charges at the interface due to a finite conductivity of one of the liquids, and/or convective processes. 2) Polarization charges in an external electric field. Apart from different electrostatic boundary conditions, several hydrodynamic models were considered, reflecting the typical experimental configurations. In addition to the surface tension, the EHD instability is either opposed by the viscous dissipation in the liquid [1,6,7], or by gravity [2–5,7].

In a thin-film geometry, research on the film stability is a field of rapidly growing activity [8], due to the fundamental interest in the interactions of liquids near surfaces, but also because of the practical relevance of film stability for a variety of applications. Commonly, film

(*) Present address: Fakultät für Physik, Universität Freiburg - D-79104 Freiburg, Germany.
(**) E-mail: u.steiner@chem.rug.nl

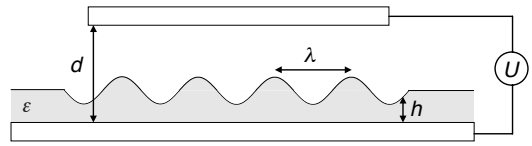

Fig. 1 – Schematic representation of the experimental setup. A liquid polymer film (gray) is destabilized by an electrostatic pressure which is a consequence of the applied electric field. Depending on the voltage U, the electrode spacing d, the initial film thickness h_0, the dielectric constant ϵ_{p}, and the surface tension γ, a narrow distribution of wavelengths λ is amplified.

instability is undesired and several strategies have been put forward to suppress the break-up of films [9]. However, the careful control of instabilities in films can be exploited to generate novel structures [10–13].

The concepts applied to describe EHD instabilities and thin-film instabilities are similar [14]. In the thin-film geometry, gravity is usually negligible and a no-slip boundary condition is assumed at the liquid-solid interfaces, giving rise to a Poiseulle-type velocity profile in the liquid layers [15].

The combination of both principles —the use of electrical fields to control the destabilization of thin polymer films— is appealing. As opposed to other interactions, the strength of electrostatic forces can be easily varied and, due to their long-ranged nature, a coupling of electrostatic interactions to dielectric interfaces far from the external surface of the specimen is possible. Recently, EHD-driven instabilities were employed to replicate a patterned electrode [13]. In related experiments, the orientation of micro-phase–separated diblock copolymers was investigated [16].

We report here a systematic characterization of an electrostatically driven instability of a thin, highly viscous polymer film. In contrast to earlier EHD experiments focusing on the threshold of the interfacial destabilization in the gravity-controlled case [4, 5], we measure the characteristic wavelength of the instability. In particular, our system allows us to precisely control all experimental parameters (see fig. 1), overcoming the difficulties in previous experiments of instabilities of surface charged polymer films [6].

The experimental setup is schematically shown in fig. 1. A thin polymer film of thickness h_0 is spin-coated from solution onto a highly polished silicon wafer serving as one of the electrodes [17]. The polymers used are listed in table I. Facing the polymer film, a second silicon wafer is mounted at a distance d from the first electrode, leaving a thin air gap $(d-h)$.

Table I – *Molecular characteristics of the polymers.*

Polymer	$M_{\mathrm{w}}^{(\mathrm{a})}$ (g/mol)	$M_{\mathrm{w}}/\mathrm{M}_{\mathrm{n}}^{(\mathrm{b})}$	$T_{\mathrm{g}}^{(\mathrm{c})}$ (°C)	$\gamma^{(\mathrm{d})}$ (mN/m)	$\epsilon^{(\mathrm{e})}$
PS	108 000	1.03	100	30.0	2.5
PMMA	98 500	1.08	105	29.7	3.6
PBrS	127 000	1.29	118	≈30	5.5

(a) Weight-averaged molecular weight.
(b) Polydispersity, with M_{n} the number-averaged molecular weight.
(c) Glass transition temperature.
(d) Surface tension. The value for PBrS is not known. We assume 30 mN/m.
(e) Dielectric constant.

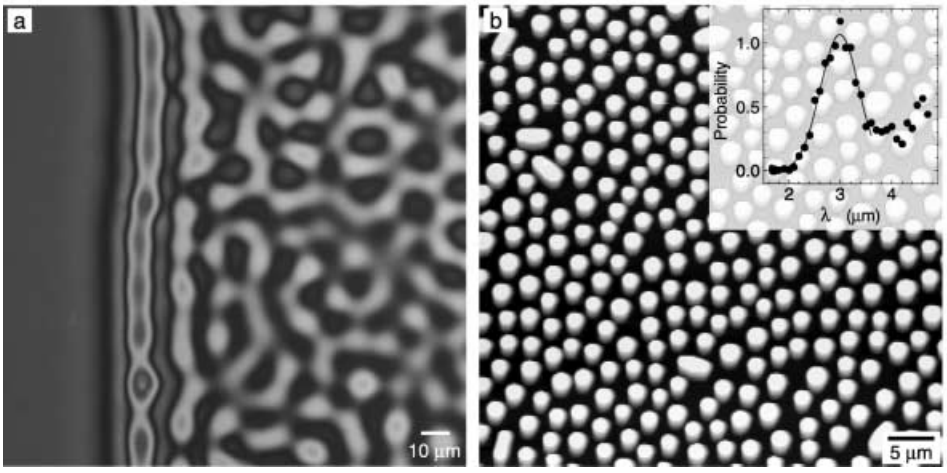

Fig. 2 – (a) Optical microscopy image of a 120 nm thick PS film annealed for 14 h at 170 °C. The right part in (a) was exposed to an electric field ($U = 50$ V, $d = 1280$ nm), showing typical modulations of the EHD instability ($\lambda = 16.3 \pm 3.3$ nm). (b) AFM image of a 115 nm thick PBrS film, annealed for 1 h at 170 °C. An applied voltage of $U = 40$ V ($d = 390$ nm) resulted in vertical columns (white) on a depleted silicon wafer (black). The inset shows the nearest-neighbor distribution of the columns with a mean of 3.0 nm and a standard deviation of 0.38 nm.

To realize a series of experiments on a single sample, a wedge geometry was used: the top electrode had a 1 μm high step, leading to a variation of d from 100 nm to 1000 nm over a lateral distance of several millimeters, thereby locally maintaining a nearly parallel electrode configuration. To facilitate a good electrical contact with the capacitor plates, the backside of the electrodes was coated with a thin gold layer. To liquify the polymer, the assembly was heated to 170 °C, above the glass transition temperature of the polymers, and a small, constant voltage U (30–50 V) was applied. The electric field in the polymer E_p and in the air gap is determined by four parameters: the voltage U, the electrode spacing d, the film thickness h_0, and the dielectric constant ϵ_p of the polymer. For the parameters used in this study, E_p was typically in the range of 10^7–10^8 V/m. During annealing with an applied voltage, a small current was flowing through the capacitor (10–50 mA/cm^2) possibly mediated by impurities in the device. After a time ranging from several minutes to a few hours, the polymer was immobilized by quenching the sample to room temperature ($T < T_\mathrm{g}$), and the top electrode was mechanically removed. To facilitate the disassembly of the device, the top electrode was covered by a self-assembled alkane monolayer [12,13] prior to the experiment. The morphology of the polymer film was investigated by optical and atomic force microscopy (AFM).

Typical experimental results are shown in fig. 2. Depending on the value of E_p and the annealing time, different stages of instability are obtained. Initially, the film shows undulations (fig. 2a). These undulations grow and eventually make contact with the upper electrode to form liquid columns (fig. 2b). Due to the wedge geometry of the sample, all stages can be obtained with the same sample for a given annealing time. Figure 2a illustrates the effect of the electric field. Here, only the right part of the sample was opposed by a counter electrode. In the absence of an electric field, the upper part of the film in fig. 2a remained stable for several hours, while the right part features a dynamic instability which is caused by the electric field. Several qualitative features emerge from fig. 2: i) the instability of the polymer is caused by the electric field [12]; ii) a narrow distribution of wavelengths is observed; and iii), as is typical

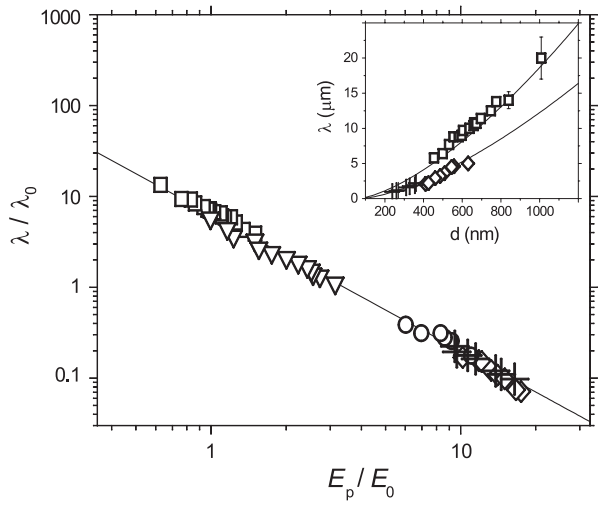

Fig. 3 – Variation of λ *vs.* the electric field in the polymer film E_p in reduced coordinates. The different symbols correspond to four data sets: □ PS with $h_0 = 93$ nm, $d = 450$–1000 nm, $U = 30$ V; ▽ PS with $h_0 = 120$ nm, $d = 600$–1730 nm, $U = 50$ V; ◯ PMMA with $h_0 = 100$ nm, $d = 230$–380 nm, $U = 30$ V; ◇ PBrS with $h_0 = 125$ nm, $d = 400$–620 nm, $U = 30$ V. The crosses correspond to an AC experiment (rectangular wave with a frequency of 1 kHz and an amplitude $U = 37$ V) using a PMMA film with $h_0 = 100$ nm, $d = 230$–360 nm. The line corresponds to eq. (6). The inset shows some of the data in non-reduced coordinates *vs.* d. Some of the data is taken from [13].

for two-dimensional systems [18] a local or global lateral hexagonal symmetry is obtained [13]. Nucleation effects are observed at impurities or at the edge of the upper electrode (fig. 2a).

Here, we will focus on the nature of the instability itself. Lateral correlations (*e.g.*, the alternating amplification of waves as seen along the edge in fig. 2a, or the threshold for hexagonal ordering) will be discussed in a forthcoming publication. To analyze the data from the AFM images and optical micrographs, we determined the characteristic wavelength λ by measuring the distances between undulation maxima or the columns and taking the average. AFM measurements provide h_0 directly after spin coating, and d is obtained from the height of the polymer columns after the experiment. To explore the effect of different ϵ_p values, three polymers were used: polystyrene (PS), polymethylmethacylate (PMMA), and brominated polystyrene (PBrS). Apart from their differing dielectric constants, all three polymers have similar properties (see table I). While the structures appear qualitatively similar for the three polymers (figs. 2a, b correspond to PS, PBrS films, respectively), it is important to point out that the characteristic wavelength decreases with increasing ϵ_p, for otherwise similar experimental parameters. This is illustrated in inset of fig. 3, where λ is plotted *vs.* d for a PS, a PMMA and a PBrS sample.

While there is an extensive body of literature on the theoretical description of the EHD instability [2,4,5,15], an adaption of the theoretical models to the boundary condition in our experiments is necessary. For an instability caused purely by polarization charges, we follow the description in [19] in the limit of $\lambda \gg d$, by adding hydrodynamic boundary conditions which lead to a half-Poiseulle flow in the viscous polymer layer [14].

The overall pressure distribution at the film surface is

$$p = p_0 - \gamma \frac{\partial^2 h}{\partial x^2} + p_\mathrm{el}\,(h) + p_\mathrm{dis}\,(h)\ , \tag{1}$$

with p_0 being the atmospheric pressure. The second term, the Laplace pressure, stems from the the surface tension γ and the fourth term, the disjoining pressure $p_{\rm dis}$, arises from dispersive van der Waals interactions. The electrostatic pressure for a given electric field in the polymer film, $E_{\rm p} = U/(\epsilon_{\rm p} d - (\epsilon_{\rm p} - 1)\, h)$, is given by $p_{\rm el} = -\epsilon_0 \epsilon_{\rm p} (\epsilon_{\rm p} - 1) E_{\rm p}^2$ [20]. For high enough values of $E_{\rm p}$, only the Laplace and electrostatic terms need to be considered. In a stability analysis, a small sinusoidal perturbation of the interface with wave number q, growth rate τ^{-1}, and amplitude u is considered: $h\,(x,t) = h_0 + u \mathrm{e}^{iqx + t/\tau}$. The modulation of h gives rise to a lateral pressure gradient inside the film, inducing a Poiseuille flow j [14]

$$j = \frac{h^3}{3\eta} \left(-\frac{\partial p}{\partial x} \right) , \tag{2}$$

where η is the viscosity of the liquid. A continuity equation enforces mass conservation of the incompressible liquid:

$$\frac{\partial j}{\partial x} + \frac{\partial h}{\partial t} = 0\,; \tag{3}$$

eqs. (1), (2) and (3) establish a differential equation that describes the dynamic response of the interface to the perturbation. In a linear approximation (to order $\mathrm{O}(u)$), a dispersion relation is obtained:

$$\frac{1}{\tau} = -\frac{h_0^3}{3\eta} \left(\gamma q^4 + \frac{\partial p_{\rm el}}{\partial h} q^2 \right) . \tag{4}$$

As opposed to the inviscid, gravity-limited case ($\tau^{-1} \propto q$) [4], the viscous stresses lead to a q^2-dependence of τ^{-1} in the long-wavelength limit, typical for dissipative systems [18]. Fluctuations are amplified if $\tau > 0$. Since $\frac{\partial p_{\rm el}}{\partial h} < 0$, all modes with $q < q_{\rm c} = \sqrt{-\frac{1}{\gamma} \frac{\partial p_{\rm el}}{\partial h}}$ are unstable. With time, the fastest growing fluctuation will eventually dominate, corresponding to the maximum in eq. (4)

$$\lambda = 2\pi \sqrt{\frac{\gamma U}{\epsilon_0 \epsilon_{\rm p} \left(\epsilon_{\rm p} - 1\right)^2}} E_{\rm p}^{-\frac{3}{2}} . \tag{5}$$

To compare the results of the dispersion relation to the experimental data, it is useful to introduce reduced variables: $\lambda_0 = \epsilon_0 \epsilon_{\rm p} (\epsilon p - 1)^2 U^2/\gamma$ and $E_0 = U/\lambda_0$. Equation (5) leads then to

$$\frac{\lambda}{\lambda_0} = 2\pi \left(\frac{E_{\rm p}}{E_0} \right)^{-\frac{3}{2}} ; \tag{6}$$

λ_0 is a characteristic length scale which is connected to the relative strength of the electrostatic and Laplace pressures. For our system, $\lambda_0 \sim 1$ μm and $E_0 \sim 10^7$ V/m, values which are comparable to the experimental results in figs. 2 and 3 (inset). In addition, eq. (4) gives a relation for the time constant of the instability: $\tau/\tau_0 = \pi^4 \left(E_{\rm p}/E_0\right)^{-6}$.

Equation (6) shows that we may rescale our data in reduced coordinates. Data sets which correspond to a range of experimental parameters superpose to a single master curve shown in fig. 3. Within the experimental scatter, the data is quantitatively described by eq. (6), in the absence of any adjustable parameters.

In the present analysis, we make the assumption that interfacial charging caused by the finite conductivity of the polymer film is negligible. To experimentally verify that only polarization effects are responsible for the EHD instability, a rectangular alternating voltage (AC) with a frequency of 1 kHz was applied at the capacitor (crosses in fig. 3), yielding results which are in good agreement with the constant voltage experiments. The absence of interfacial charging is, however, in disagreement with the discussion in [5], which estimates a characteristic

time for charge transport of ∼20 s (assuming a conductivity of PS of 10^{-12} $(\Omega\mathrm{m})^{-1}$). On the other hand, the observed current may discharge the polymer surface.

As opposed to the gravity-controlled case, there is no lower threshold field for the EHD instability in our case, due to the dissipative character of the viscous drag that opposes the destabilizing electrostatic force. In practice, other destabilizing contributions to the pressure balance in eq. (1) have to be considered for low values of p_{el}, such as dispersion forces, nucleation effects, etc.

In conclusion, we have presented an experimental study on the EHD instability in thin, highly viscous polymer films. A comparison of the data with (slightly modified) EHD theories allows us to collapse all our data onto a master curve which is well described by the model without adjustable parameters. Our experiment provides precise control over all experimental parameters. It allows a detailed observation of all stages of the EHD instability resulting in an analysis of the EHD morphology of unprecedented clarity. EHD experiments with thin polymer films are a model system to study instabilities caused purely by polarization charges. They are also ideally suited to study non-equilibrium pattern formation in two dimensions [18]. In addition, the use of externally applied fields may be a useful tool to experimentally verify whether electrostatic effects contribute to the instability and dewetting of thin liquid films [15].

* * *

We thank J. Mlynek for his support, S. Walheim and Ph. Maass for helpful discussions and S. Harkema for his help with the experiments, W. Zulehner and Wacker-Chemie GmbH for the silicon wafers, and C. Hawker for the brominated polystyrene. This work was funded by the Deutsche Forschungs Gemeinschaft (DFG) through the Sonderforschungsbereich 513, the Dutch "Stichting voor Fundamenteel Onderzoek der Materie" (FOM), NATO, the US Department of Energy and the National Science Foundation through the Materials Research Science and Engineering Center.

REFERENCES

[1] Swan J. W., *Proc. R. Soc. (London)*, **62** (1897) 38.
[2] Tonks L., *Phys. Rev.*, **48** (1935) 562; Frenkel J., *Phys. Z. Sowjetunion*, **8** (1935) 675.
[3] Leiderer P., *Two-Dimensional Electron Systems*, edited by E. Y. Andrei (Kluwer) 1997, p. 317.
[4] Melcher J. R., *Phys. Fluids*, **4** (1961) 1348; *Field-Coupled Surface Waves* (MIT Press, Cambridge, Mass.) 1963); Taylor G. I. and McEwan A. D., *J. Fluid Mech.*, **22** (1965) 1; Melcher J. R. and Smith C. V., *Phys. Fluids*, **8** (1969) 1193.
[5] Reynolds M., *Phys. Fluids*, **8** (1965) 161.
[6] Glen W. E., *J. Appl. Phys.*, **30** (1959) 1870; Killat U., *J. Appl. Phys.*, **46** (1975) 5169.
[7] Néron de Surgy G., Chabrerie J.-P., Denoux O. and Wesfreid J.-E., *J. Phys. II*, **3** (1993) 1201.
[8] Brochard F., de Gennes P.-G., Hervet H. and Redon C., *Langmuir*, **10** (1994) 1566; Reiter G., *Phys. Rev. Lett*, **68** (1992) 75; Sharma A. and Reiter G., *J. Colloid Interface Sci.*, **178** (1996) 383; Jacobs K., Herminghaus S. and Mecke K., *Langmuir*, **14** (1998) 965.
[9] Yerushalmi-Rosen R., Klein J. and Fetters L., *Science*, **263** (1994) 793.
[10] Böltau M., Walheim S., Mlynek J., Krausch G. and Steiner U., *Nature*, **391** (1998) 877.
[11] Chou S., Zhuang L. and Guo L., *Appl. Phys. Lett.*, **75** (1999) 1004.
[12] Chou S. and Zhuang L., *J. Vac. Technol. B*, **17** (1999) 3197.
[13] Schäffer E., Thurn-Albrecht T., Russell T. P. and Steiner U., *Nature*, **403** (2000) 874.
[14] Vrij A., *Discuss. Faraday Soc.*, **42** (1966) 23.

[15] Herminghaus S., *Phys. Rev. Lett.*, **83** (1999) 2359.
[16] Amundson K., Helfand E., Quan X., Hudson S. and Smith S., *Macromolecules*, **27** (1994) 6559; Morkved T., Lu M., Urbas A., Ehrichs E., Jaeger H., Mansky P. and Russell T. P., *Science*, **273** (1996) 931; Thurn-Albrecht T., DeRouchey J., Russell T. P. and Jaeger H., *Macromolecules*, **33** (2000) 3250.
[17] The silicon wafers (donated by Wacker-Chemie GmbH) had a ($\approx$ 2 nm thick) native oxide layer. Prior to the deposition of the polymer film, the wafers were cleaned using a "snow-jet" (Sherman R., Hirt D. and Vane R. J., *J. Vac. Sci. Technol.*, **12** (1994) 1876). The cleaned silicon oxide surfaces had a water contact angle of less than 10° and were completely wetted by all polymers used in this study.
[18] Cross M. C. and Hohenberg P. C., *Rev. Mod. Phys.*, **65** (1993) 851.
[19] Onuki A., *Physica A*, **217** (1995) 38.
[20] When deriving p_{el}, two contributions to the free-energy change have to be considered: i) the redistribution of dielectric liquid inside the capacitor and ii) additional dielectric liquid which is drawn into the capacitor from an outside reservoir.